

The 1:±2 resonance

R.H. Cushman^{1,3}, Holger R. Dullin², Heinz Hanßmann¹, Sven Schmidt²

¹ Mathematisch Instituut, Universiteit Utrecht,
Postbus 80.010, 3508 TA Utrecht, The Netherlands

² Department of Mathematical Sciences,
Loughborough University, LE11 3TU, UK

H.R.Dullin@lboro.ac.uk

³ Department of Mathematics and Statistics,
University of Calgary, Canada

October 1, 2007

Abstract

On the linear level elliptic equilibria of Hamiltonian systems are mere superpositions of harmonic oscillators. Non-linear terms can produce instability, if the ratio of frequencies is rational and the Hamiltonian is indefinite. In this paper we study the frequency ratio $\pm 1/2$ and its unfolding. In particular we show that for the indefinite case (1:−2) the frequency ratio map in a neighbourhood of the origin has a critical point, i.e. the twist condition is violated for one torus on every energy surface near the energy of the equilibrium. In contrast, we show that the frequency map itself is non-degenerate (i.e. the Kolmogorov non-degeneracy condition holds) for every torus in a neighbourhood of the equilibrium point. As a by product of our analysis of the frequency map we obtain another proof of fractional monodromy in the 1:−2 resonance.

1 Introduction

The problem of resonant equilibria in Hamiltonian systems is quite intricate. The set of resonant frequencies is countable and dense within all frequencies. It is therefore generic for a Hamiltonian system to have all equilibria non-resonant, but the set of all such Hamiltonians is not open. An approach that allows to recover an open and dense set of Hamiltonians is to make a distinction between resonances of high and low order. The latter concern equilibria with local dynamics significantly different from that of any *Birkhoff normal form*. In two degrees of freedom this makes the 0:0, 0:1, 1:±1, 1:±2 and 1:±3 resonances low order resonances. For high order resonances the local dynamics is essentially governed by a Birkhoff normal form, cf. [30].

Thus it requires an external parameter λ to encounter a resonant equilibrium in a Hamiltonian system. The rôle of λ is to detune the frequencies. In fact, the 0:0 resonance — an equilibrium with nilpotent linearization — is of co-dimension 2 and needs generically one detuning parameter for each of the two frequencies, cf. [8]. The 1:1 resonance is special as well : already the linear centraliser unfolding needs 3 detuning parameters. In [7] a universal unfolding of the full (nonlinear) problem with 7 parameters is computed. The 0:1 and 1:−1 resonances lead under parameter variation to hyperbolic eigenvalues. This triggers the normally elliptic centre–saddle (or Hamiltonian saddle–node) bifurcation [4] and the Hamiltonian Hopf bifurcation [33], respectively.

In this paper we consider both the 1:2 and the 1:−2 resonance ; we use the notation $\sigma = \pm 1$ in order to treat these cases in a parallel fashion. Moving the resonant equilibrium to both the origin $(q, p) = 0$ of the phase space \mathbb{R}^4 and the origin of parameter space to $\lambda = 0$, the linear part of the Hamiltonian vanishes and the quadratic part at the resonance reads

$$H_2(q, p) = \frac{\omega}{2} [p_1^2 + q_1^2 + 2\sigma(p_2^2 + q_2^2)] .$$

The eigenvalues are $\pm i\omega, \pm 2i\omega$ and thus in 1: ± 2 resonance. We scale the frequency ω to 1 by a linear change of time. The linear centraliser unfolding

$$G_2(q, p; \lambda) = \frac{1}{2}(p_1^2 + q_1^2) + \sigma(p_2^2 + q_2^2) + \frac{\lambda}{2}(p_1^2 + q_1^2)$$

consists in adding a convenient detuning term.

Our interest lies in the full nonlinear dynamics defined by a family $H(q, p; \lambda)$ of Hamiltonians with quadratic part G_2 . In addition to the linear terms we also set the constant term equal to zero. Thus we are confronted with

$$H(q, p; \lambda) = G_2(q, p; \lambda) + G_3(q, p; \lambda) + G_4(q, p; \lambda) + \dots \quad (1.1)$$

where G_k is a homogeneous polynomial of order k in (q, p) that may have λ -dependent coefficients. Close to the origin G_k dominates G_l for $k < l$ and we claim that already the cubic polynomial

$$H_3(q, p; \lambda) = G_2(q, p; \lambda) + G_3(q, p; \lambda)$$

contains the desired information, provided that the average \overline{G}_3 of G_3 over the periodic flow of X_{H_2} does not vanish at $\lambda = 0$. Indeed, our first step will be to derive a normal form

$$\overline{H}_3(q, p; \lambda) = G_2(q, p; \lambda) + \overline{G}_3(q, p; \lambda). \quad (1.2)$$

Note that this would also be the first step to compute a Birkhoff normal form, for which the terms of odd order vanish. Because of the resonance we have an unremoveable odd order term. The result is called resonant Birkhoff normal form.

In case \overline{G}_3 does vanish identically we may proceed to compute the Birkhoff normal form up to order 4, and for non-degenerate quartic terms this special 1: ± 2 resonance becomes a high order resonance. The tricky bit is when \overline{G}_3 does vanish at $\lambda = 0$, but not identically in λ . This case is of co-dimension 2 and one would then use a coefficient c in \overline{G}_3 as second unfolding parameter.

By construction the normal form Hamiltonian (1.2) is invariant under the periodic flow generated by H_2 . Our second step consists in the reduction of this S^1 -symmetry. The origin $(q, p) = 0$ is fixed whence S^1 does not act freely and we have to resort to singular reduction [9]. This reduction is performed by choosing a *Hilbert basis* $\{\pi_1, \pi_2, \pi_3, \pi_4\}$, *i.e.* generators of the ring of S^1 -invariant functions as (global) co-ordinates. A certain drawback is that this basis is not free, whence we have to work on the 3-dimensional semi-algebraic subvariety of \mathbb{R}^4 that is defined by

$$\pi_1^2 \pi_2 = \pi_3^2 + \pi_4^2, \quad \pi_1 \geq 0, \quad \pi_2 \geq 0. \quad (1.3)$$

The normal form \overline{H}_3 induces a Hamiltonian \mathcal{H} on this reduced phase space. Being of one degree of freedom the corresponding reduced Hamiltonian system is readily analysed. We do this both globally on the symplectic leaves of the reduced phase space and locally in well-chosen co-ordinates. See Elipe et al [18, 19] for a similar approach in the setting of stability analysis. Due to the geometry of the reduced phase space, it is convenient to plot the energy surface in the space of the invariants (figures 2 and 3). This technique was, in fact, already known to Alfried [1] and even earlier to Breakwell and Pringle [2].

Our third step concerns the dynamics in two degrees of freedom. This consists of two parts. First we reconstruct the dynamics defined by the normal form \overline{H}_3 from the reduced Hamiltonian \mathcal{H} . In the case $\sigma = +1$ of the 1:2 resonance this makes \mathbb{R}^4 a *ramified torus bundle*, with regular fibres \mathbb{T}^2 reconstructed from the periodic orbits of the reduced system. In the case $\sigma = -1$ of the 1:-2 resonance the reduced system always has unbounded motion. It may also have bounded orbits depending on the detuning. We show by a direct computation that \mathbb{R}^4 becomes a ramified fibre bundle, where the regular fibres are 2-tori and cylinders reconstructed from bounded and unbounded orbits, respectively, in the pre-image of the regular values of the energy-momentum mapping. In order to give a global overview of the dynamics we then go on and construct in both cases $\sigma = \pm 1$ the sets of critical values of the energy-momentum mappings.

The fourth step relates the reconstructed integrable dynamics defined by (1.2) to the ‘‘original’’ dynamics defined by (1.1). For $\sigma = +1$ this perturbation analysis is straightforward. Things turn out to be more interesting for the 1:-2 resonance. Indeed, we show that the ramified fibre bundle defined by (1.2) displays

fractional monodromy around the singular fibre containing the origin $(q, p) = 0$ (in the case $\sigma = +1$ the corresponding singular fibre consists of the origin alone). This phenomenon is treated in Section 5. The main technical issue is to define the notion of frequency and frequency ratio (which shows monodromy) for the non-compact cylinders. The approach taken in [17] is to add higher order terms to the Hamiltonian that make the energy surface compact. We follow a different approach along the lines of [29] where only the singular part of the dynamics near the equilibrium point is considered. This singular part captures the dynamics up to a smooth (but unknown) function that encode the influence of higher order terms. However, the singular terms dominate the asymptotic behaviour of the frequency map when sufficiently close to the equilibrium, and thus nothing needs to be known about the higher order terms, except their existence and smoothness.

The unfolding shows that our situation is different from the unfolded 1:−1 resonance. When passing through a 1:−1 resonance, (non-fractional) monodromy is created in a supercritical Hamiltonian Hopf bifurcation and local monodromy is turned into non-local [34] island [16] monodromy in the subcritical case. The situation is different for the 1:−2 resonance (where no distinction super/subcritical exists). Fractional monodromy [28] is local at $\lambda = 0$ and turns into island monodromy for both positive and negative values of λ . Stated differently, the system has fractional monodromy before and after resonance. When passing through a 1:−2 resonance island monodromy momentarily contracts to local monodromy.

In the final section we come to our main new results on the 1:−2 resonance. We show that the isoenergetic non-degeneracy (or twist) condition is violated for a single torus on every energy near the critical energy. This shows that the principle “low order resonance leads to vanishing twist” (already established for low order resonant fixed points of maps [14, 12]) is also valid for low order resonant equilibria. This shows that the principle “monodromy causes vanishing twist”, which has been established for the Hamiltonian Hopf bifurcation [13] and for focus-focus equilibria in general [15] also holds in the more degenerate (and more difficult) situation of the 1:−2 resonance. The second main new result is that the frequency map for tori near the 1:−2 equilibrium is non-degenerate, i.e. the Kolmogorov condition for the KAM theorem holds. Again, this is similar to the situation for focus-focus points [15]. The main difference with the focus-focus equilibrium is that this equilibrium was assumed to be non-degenerate (in the sense that the linearisation of the commuting vector fields generate the Cartan sub-algebra); whereas in the 1:−2 equilibrium it is always degenerate. Our analysis shows that this implies that the period only has algebraic blowup, as opposed to the usual logarithmic one.

Our results are valid for all completely integrable systems that agree up to the cubic terms with the normal form we analyse. The higher order terms do not change the asymptotic properties of the frequency map when sufficiently close to the origin. An arbitrary Hamiltonian system near the 1 : −2 resonance is generically non-integrable due to higher order terms. Thus it does not possess a frequency map. Using our results about the non-degeneracy of the frequency map, then KAM theory can be invoked to show the persistence of tori whose frequencies are Diophantine. Moreover, monodromy can be defined for the nearby non-integrable system [3].

2 Normal form

The art of normalizing Hamiltonian Systems has been periodically (re)discovered and forgotten and goes at least back to Birkhoff. For treatments similar to ours see *e.g.* [33, 5, 13]. The resonant quadratic part H_2 generates the S^1 -action

$$\varrho : S^1 \times \mathbb{C}^2 \longrightarrow \mathbb{C}^2 \\ (t, z_1, z_2) \longmapsto (z_1 e^{it}, z_2 e^{2\sigma it})$$

where $z_k = (p_k + iq_k)/\sqrt{2}$, $k = 1, 2$. Introducing

$$z_2^\sigma = \begin{cases} \bar{z}_2 & \text{if } \sigma = +1 \\ z_2 & \text{if } \sigma = -1 \end{cases}$$

this action has the invariants

$$\pi_1 = z_1 \bar{z}_1, \quad \pi_2 = z_2 \bar{z}_2, \quad \pi_3 = \operatorname{Re}(z_1^2 z_2^\sigma), \quad \pi_4 = \operatorname{Im}(z_1^2 z_2^\sigma).$$

These form a Hilbert basis of the ring $(C(\mathbb{R}^4))^{\varrho}$ of ϱ -invariant functions, *i.e.* given a ϱ -invariant function $f : \mathbb{R}^4 \rightarrow \mathbb{R}$ there exists $g : \mathbb{R}^4 \rightarrow \mathbb{R}$ such that

$$f(q, p) \equiv g(\pi(q, p)) .$$

Normalization of $H(q, p; \lambda)$ with respect to this action gives a Hamiltonian that is a function of the invariants only. The only cubic polynomial that is a polynomial of the invariants is the linear combination $a\pi_3 + b\pi_4$. A simultaneous rotation in both the (q_1, p_1) -plane and the (q_2, p_2) -plane turns this expression into $c\pi_3$ with $c^2 = a^2 + b^2$. Unless $c = 0$ we assume that $c > 0$. This yields the following result [11, 25].

Theorem 1. *Let the family $H(q, p; \lambda)$ of two-degree-of-freedom Hamiltonian systems be given by (1.1), *i.e.* with quadratic part unfolding the 1:±2 resonance. Then there is a symplectic co-ordinate transformation ψ that turns $H(q, p; \lambda)$ into normal form*

$$(H \circ \psi)(q, p; \lambda) = G_2(q, p; \lambda) + \overline{G}_3(q, p; \lambda) + \text{higher order terms}$$

with $\overline{G}_3(q, p; \lambda) = c(\lambda) [(p_1^2 - q_1^2)p_2 + 2\sigma p_1 q_1 q_2]$.

Introducing the scaling $(q, p, H) \mapsto (\varepsilon q, \varepsilon p, \varepsilon^2 H)$ zooms into the origin and reveals the smallness of the higher order terms as the normal form reads

$$(H \circ \psi)(q, p; \lambda) = G_2(q, p; \lambda) + \varepsilon \overline{G}_3(q, p; \lambda) + \mathcal{O}(\varepsilon^2) .$$

Restricting to a small interval $]-\lambda_0, \lambda_0[$ in parameter space defined by

$$c(\lambda) \equiv c(0) + \mathcal{O}(\varepsilon)$$

we may furthermore put $c(\lambda) \equiv c(0) =: c$ in \overline{G}_3 whence the normal form (1.2) turns out to be an ε^2 -small perturbation of (1.1). Note that if $c'(0) \neq 0$, then $\lambda_0 = \mathcal{O}(\varepsilon)$, Therefore we may rescale $\lambda \mapsto \varepsilon \lambda$ as well. This turns (1.2) into

$$\begin{aligned} \overline{H}_3(q, p; \lambda) &= \frac{1}{2}(p_1^2 + q_1^2) + \sigma(p_2^2 + q_2^2) \\ &+ \varepsilon \left\{ \frac{\lambda}{2}(p_1^2 + q_1^2) + c[(p_1^2 - q_1^2)p_2 + 2\sigma p_1 q_1 q_2] \right\} . \end{aligned}$$

From now on we assume that the non-degeneracy condition $c > 0$ holds. The additional scaling $(\lambda, \varepsilon) \mapsto (\lambda c, c^{-1}\varepsilon)$ would yield $c = 1$. We keep c in the calculation so that we can absorb additional constants when they appear. Moreover, later on we want to (re)-introduce the scaling in a slightly different way in the image of the energy-momentum map.

3 Reduction

The normalized truncated cubic Hamiltonian is Liouville integrable with integral H_2 . The flow generated by H_2 is periodic, and hence it is the momentum of an S^1 -action. Singular reduction of this symmetry gives a system with one degree of freedom. Instead of working with $\pi_1, \pi_2, \pi_3, \pi_4$ it is convenient to use a slightly different Hilbert basis of the ring $(C(\mathbb{R}^4))^{\varrho}$ of ϱ -invariant functions that contains the generator of the S^1 action. Therefore we drop π_2 in favour of

$$\eta = \pi_1 + 2\sigma\pi_2 = \frac{1}{2}(p_1^2 + q_1^2) + \sigma(p_2^2 + q_2^2)$$

Whence the relation between the invariants reads $R_\eta(\pi_1, \pi_3, \pi_4) = 0$ with

$$R_\eta(\pi_1, \pi_3, \pi_4) = \frac{\sigma}{2}\pi_1^2(\eta - \pi_1) - (\pi_3^2 + \pi_4^2);$$

while the inequalities $\pi_1 \geq 0, \pi_2 \geq 0$ turn into an interval \mathcal{I}_η of admissible values for π_1 . In the case $\sigma = +1$ of the 1:2 resonance this interval is bounded and given by

$$\mathcal{I}_\eta^+ = [0, \eta];$$

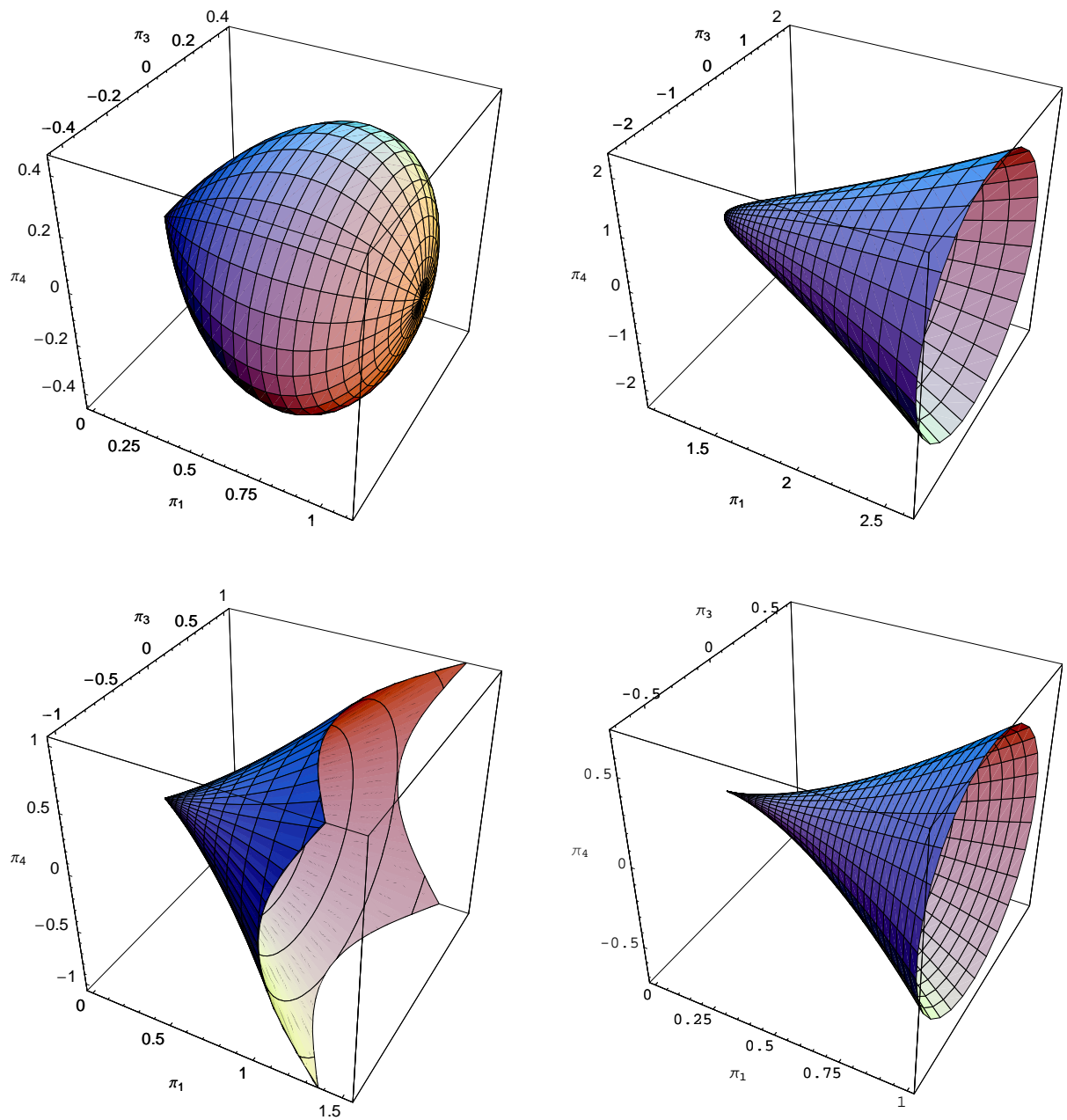


Figure 1: The reduced phase spaces that occur in the $1 : \pm 2$ resonance. Upper left: $\sigma = +1$ and $h_2 > 0$ (not shown: $P_{h_2}^\sigma = \emptyset$ for $\sigma = +1$ and $h_2 < 0$ and $P_0^+ = \{0\}$); upper right: $\sigma = -1$ and $h_2 > 0$, lower left: $\sigma = -1$ and $h_2 < 0$ and lower right: $\sigma = -1$ and $h_2 = 0$.

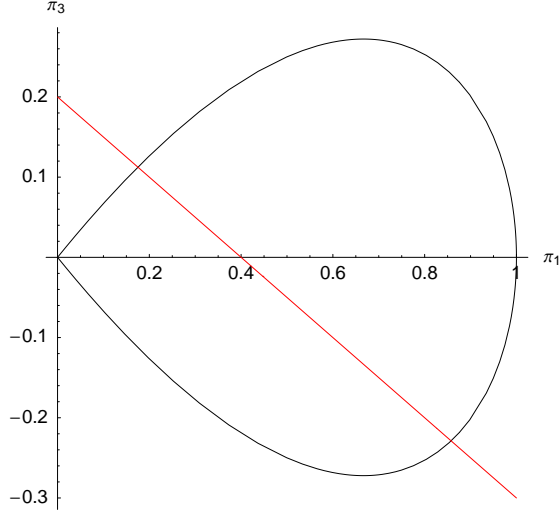


Figure 2: Section $\pi_4 = 0$ and $\pi_1 + 2\pi_2 = h_2$ of the reduced phase space for $\sigma = +1$, $h_2 = 1$, together with a line of constant Hamiltonian $h = h_2 + \lambda\pi_1 + c\pi_3 = 1.2$, $\lambda = 1/2$, $c = 1$.

whereas for $\sigma = -1$, the invariant η may assume negative values as well and

$$\mathcal{I}_\eta^- = [\max\{0, \eta\}, \infty[$$

is unbounded. The Poisson bracket relations between the invariants are easily computed and given in table 1, where

$$f(\pi_1) = \frac{\sigma}{2}(2\eta\pi_1 - 3\pi_1^2) = \frac{\partial R_\eta}{\partial \pi_1}.$$

Because η coincides with H_2 it was to be expected that this invariant is a Casimir of the reduced Poisson structure.

Table 1: The reduced Poisson bracket.

$\{\uparrow, \leftarrow\}$	π_1	π_3	π_4	η
π_1	0	$2\pi_4$	$-2\pi_3$	0
π_3	$-2\pi_4$	0	$f(\pi_1)$	0
π_4	$2\pi_3$	$-f(\pi_1)$	0	0
η	0	0	0	0

Fixing the value h_2 of η the one-degree-of-freedom dynamics takes place in the surface of revolution (see figure 1)

$$P_{h_2}^\sigma = \{ (\pi_1, \pi_3, \pi_4) \in \mathbb{R}^3 \mid R_{h_2}(\pi_1, \pi_3, \pi_4) = 0, \pi_1 \in \mathcal{I}_{h_2}^\sigma \}$$

with Poisson structure

$$\{f, g\} = (\nabla f \times \nabla g \mid \nabla R_\ell).$$

Note that $P_{h_2}^+$ is compact and $P_{h_2}^-$ is unbounded. The conical singular point at $\pi_1 = 0$ (unless $\sigma = -1$ and $h_2 > 0$) comes from the isotropy subgroup \mathbb{Z}_2 of the S^1 -action ρ at $(0, z_2)$. When $\sigma = -1$, such points satisfy $h_2 \leq 0$.

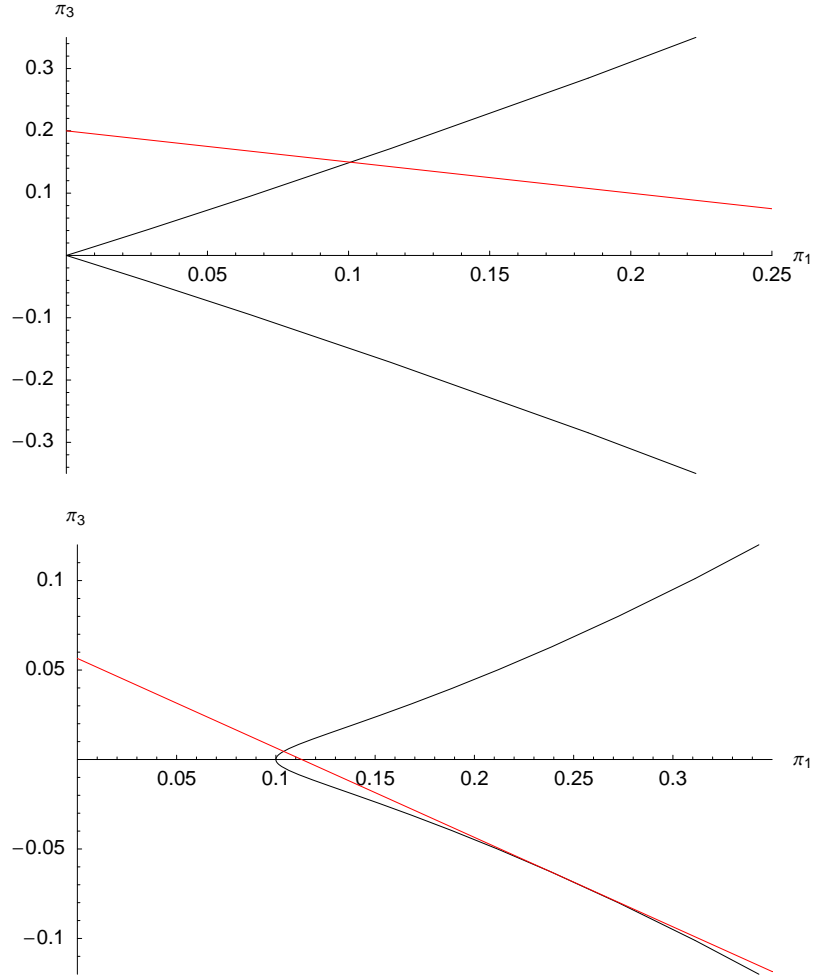


Figure 3: Section $\pi_4 = 0$ and $\pi_1 - 2\pi_2 = h_2$ of the non-compact reduced phase space for $\sigma = -1$. For $h_2 = -1$ (top), there is a singular point at the origin. The line of constant Hamiltonian is determined by $\Delta h = 0.2$, $\lambda = 1/2$, $c = 1$. For $h_2 = 0.1$ (bottom), the reduced phase space is smooth. The line of constant Hamiltonian is given by $\Delta h = 0.0565$, $\lambda = 1/2$, $c = 1$.

The reduced Hamiltonian is obtained by expressing \overline{H}_3 in the basic invariants and reads

$$\mathcal{H}_3(\pi_1, \pi_3, \pi_4; \lambda) = \eta + \varepsilon \{ \lambda \pi_1 + c \pi_3 \}, \quad (3.4)$$

where the factor $2\sqrt{2}$ has been absorbed in the factor c . Subtracting the constant value h_2 of η and rescaling time by ε yields

$$\mathcal{H}(\pi_1, \pi_3, \pi_4; \lambda) = \lambda \pi_1 + c \pi_3.$$

It is important to keep in mind that subtracting h_2 is only a valid operation in the reduced system, but not in the full system. Altering the Hamiltonian by a constant in general makes no difference to the dynamics. Eventhough H_2 is constant along trajectories of the full averaged system, it does contribute leading order terms to the equations of motion, and thus influences the frequencies and rotation number. In the reduced system the function η (with value h_2) is a Casimir of the reduced bracket. Hence removing it does not change the equations of motion. So even though in the unreduced system we should not remove H_2 , we will see that the fractional monodromy is created by the non-linear terms \overline{G}_3 , and the monodromy is not changed by removing H_2 .

The reduced integral curves are given by the intersections

$$P_{h_2}^\sigma \cap \mathcal{H}^{-1}(\Delta h),$$

where $\Delta h = h - h_2$ is the difference between the value h of the energy and the value h_2 of η , i.e. the value of the cubic terms in the Hamiltonian. In addition to the singular points, we have regular equilibria where $\mathcal{H}^{-1}(\Delta h)$ is tangent to $P_{h_2}^\sigma$. Because the latter is a surface of revolution and the former is a plane parallel to the π_4 -axis this requires $\pi_4 = 0$. Hence, we merely have to compute the points where the straight line

$$\pi_3 = \frac{\Delta h}{c} - \frac{\lambda}{c} \pi_1$$

is tangent to the cubic curve when $\pi_1 \in \mathcal{I}_{h_2}^\sigma$ and

$$\pi_3^2 = \frac{\sigma}{2} \pi_1^2 (\eta - \pi_1), \quad (3.5)$$

see figures 2 and 3. When this happens at the singular point $\pi_1 = 0$, a Hamiltonian flip bifurcation occurs as h_2 is varied, cf. [21]. In the full system this corresponds to a supercritical period-doubling bifurcation. This explains the phase portraits when $\sigma = +1$. For $\sigma = -1$ the subcritical Hamiltonian flip bifurcation at the singular equilibrium for $h_2 < 0$ is accompanied by a centre-saddle bifurcation (of regular equilibria) for $h_2 > 0$, both emanating from the non-conical singularity $\pi_1 = 0$ at $\lambda = 0$. This is best illustrated in terms of the critical values in the image of the energy-momentum map, see below.

3.1 Rational Parametrisation

An interesting feature of the $1:\pm 2$ resonances is that the two semi-algebraic varieties $P_{h_2}^+$ and $P_{-h_2}^-$ together form the cubic $R_{h_2}^{-1}(0)$. Only when $h_2 < 0$ the reduced phase space $P_{h_2}^+$ is empty and the cubic $R_{h_2}^{-1}(0)$ has an additional isolated point at the origin. Since this cubic always has a singular point there exists a rational parametrisation given by

$$(\pi_1, \pi_3)(s) = (h_2 - 2\sigma s^2, s\pi_1)$$

where $s = \pi_3/\pi_1$ is the slope of the line through the origin that intersects the cubic at (π_1, π_3) . Similarly there is an explicit polynomial parametrisation using the inhomogeneous co-ordinates $s_1 = \pi_3/\pi_1$ and $s_2 = \pi_4/\pi_1$ such that

$$(\pi_1, \pi_2, \pi_3, \pi_4)(s_1, s_2) = (h_2 - 2\sigma(s_1^2 + s_2^2), s_1^2 + s_2^2, s_1\pi_1, s_2\pi_1).$$

This stereographic projection from the singular point onto the plane $\pi_1 = 1$ gives co-ordinates on the reduced phase space. Here (π_1, π_3, π_4) are like homogeneous co-ordinates, while s_1, s_2 are inhomogeneous co-ordinates on the plane $\pi_1 = 1$. A similar construction can be done with the plane $\pi_2 = 1$.

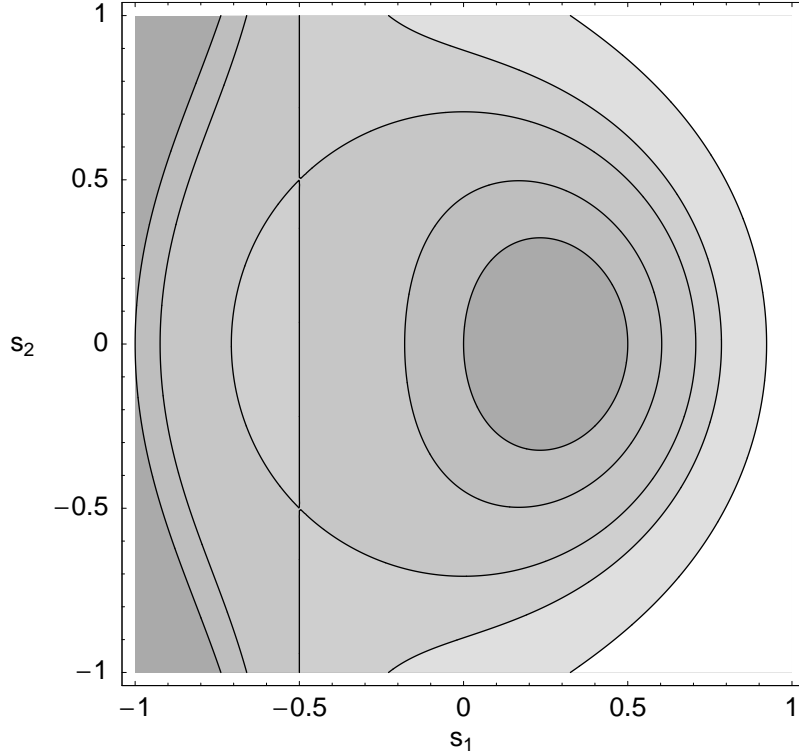


Figure 4: Phase portrait of $\mathcal{H}(s; \lambda)$ for $\sigma = \pm 1$, $h_2 = \pm 1$, $\lambda = 1/2$, $c = 1$.

Theorem 2. *The inhomogeneous co-ordinates $(s_1, s_2) = (\pi_3/\pi_1, \pi_4/\pi_1)$ are symplectic co-ordinates (up to a multiplier) on the singular reduced phase space:*

$$\{s_1, s_2\} = \frac{\sigma}{2}.$$

The reduced Hamiltonian $\mathcal{H}(\pi; \lambda) = \lambda\pi_1 + c\pi_3$ in these co-ordinates is

$$\mathcal{H}(s; \lambda) = (\lambda + cs_1)(h_2 - 2\sigma(s_1^2 + s_2^2)).$$

Proof. By direct calculation. □

The level lines of $\mathcal{H}(s; \lambda)$ define the planar phase portrait, see figure 4 for an example. The singular point of the reduced phase space (in π_i) is blown up to the invariant circle $h_2 = \sigma(s_1^2 + s_2^2)$ in the phase portrait. If the line $s_1 = -\lambda/c$ intersects the circle it contains two equilibrium points. For $\sigma = 1$ the relevant part of the phase portrait is the closed disk inside this circle, while for $\sigma = -1$ and $h_2 < 0$ it is the closure of the complement. Recall that the two reduced phase spaces for $\sigma h_2 > 0$ are just different parts of the same singular cubic curve, and in the same way the union of the two phase portraits gives all of the plane $\mathbb{R}^2 = \{s_1, s_2\}$.

When there is no singular point in the reduced phase space, $\sigma h_2 < 0$, the phase portrait is all of $\mathbb{R}^2 = \{s_1, s_2\}$. The circle seen in the case $\sigma h_2 > 0$ now has negative radius.

The other prominent feature of the phase portrait is the invariant line $s_1 = -\lambda/c$. It is the image of the energy surface $\Delta h = 0$, which is a plane through the origin $0 = \lambda\pi_1 + c\pi_3$ intersected with the reduced phase space. When $\sigma h_2 > 0$ this line is the pre-image of the critical value. If this line intersects the critical circle, then the equilibrium is unstable and the line is the separatrix. If the line and the circle do not intersect, or if there is no circle ($\sigma h_2 < 0$), then the line does not contain critical points, see Haller and Wiggins [20].

4 Dynamics in two degrees of freedom

To reconstruct the dynamics of \overline{H}_3 , we have to attach a 1–torus S^1 to every regular point of $P_{h_2}^\sigma$. In this way the periodic orbits in $P_{h_2}^\sigma$ give rise to invariant 2–tori and the unbounded reduced motions that exist for $\sigma = -1$ give rise to invariant cylinders; while regular equilibria lead to periodic orbits in \mathbb{R}^4 . For the singular equilibria the isotropy group becomes important. The singular equilibria $(\pi_1, \pi_2, \pi_3, \pi_4) = (0, h_2/(2\sigma), 0, 0) \in P_{h_2}^\sigma$ with $h_2 \neq 0$ lead to periodic orbits as well, albeit with half the period. From the singular equilibria $\pi_1 = 0$, we reconstruct the initial equilibrium at the origin of \mathbb{R}^4 .

The bifurcations of equilibria of the reduced system translate to bifurcations of periodic orbits in two degrees of freedom. The centre–saddle bifurcation turns straightforwardly into a periodic centre–saddle bifurcation. Where the singular equilibrium undergoes a Hamiltonian flip bifurcation we obtain a period–doubling bifurcation, supercritical (new orbit is elliptic) for $\sigma = +1$ and subcritical (new orbit is hyperbolic) for $\sigma = -1$. Note that in the latter case the (hyperbolic) periodic orbit with twice the period bifurcates off from the \mathbb{Z}_2 –isotropic one as h_2 increases through negative values (*i.e.* $|h_2|$ decreases), while the elliptic periodic orbit with twice the period comes into existence as h_2 increases through positive values.

In the latter case $\sigma = +1$ of the 1:2 resonance the periodic orbits are elliptic and the regular fibres of the energy–momentum mapping $\mathcal{EM} = (H_2, \overline{H}_3)$ are compact. Whence the foliation into 2–tori is locally trivial and the pre–image $\mathcal{EM}^{-1}(\bigcup \rho) \subseteq \mathbb{R}^4$ of regular values ρ of \mathcal{EM} is a 2–torus bundle. In the hyperbolic case the periodic orbits together with their (un)stable manifolds, determine the structure of this bundle. Together they turn the phase space \mathbb{R}^4 into a ramified 2–torus bundle. A similar result for the case $\sigma = -1$ does not follow from general theorems. We therefore show by direct computation that the 1:–2 resonance turns the phase space into a ramified cylinder bundle. With detuning there are some compact tori as well.

4.1 Local triviality

Because $h = \Delta h + h_2$ is linear in π_3 we can eliminate π_3 from the relation $R_{h_2} = 0$. To this end we define the polynomial

$$Q(z) = 2\sigma c^2 z^2 (h_2 - z) - 4(\Delta h - \lambda z)^2, \quad (4.6)$$

whence $\pi_4^2 = Q(\pi_1)/(4c^2)$. This is an elliptic curve, and can be parametrised by elliptic functions. Thus assume we have $(\pi_1(s; f), \pi_4(s; f))$ where $s \in \mathbb{R}$ is the parameter and $f = (h_2, \Delta h)$ denotes the values of the energy–momentum mapping. By the foregoing analysis we know that the curve is not compact, but smooth when f is a regular value. By back–substitution we find

$$\begin{aligned} \pi_2(s, f) &= \frac{\sigma}{2}(h_2 - \pi_1(s; f)) \\ \pi_3(s; f) &= \frac{1}{c}(h - h_2 - \lambda\pi_1(s; f)). \end{aligned}$$

Next we need to find a point (q, p) in phase space, so that the reduction mapping $(q, p) \mapsto (\pi_1, \pi_2, \pi_3, \pi_4)$ sends it to given values of the invariants. If such a mapping exists, we have a section of the bundle defined by the energy momentum mapping in a neighbourhood of a regular value. This mapping is

$$(p_1, q_1, p_2, q_2) = \left(\sqrt{\pi_1}, 0, \frac{\pi_3}{\pi_1}, -\sigma \frac{\pi_4}{\pi_1} \right),$$

which is well defined because for regular values of f the invariant π_1 is nonzero (and positive in any case). Finally, since the S^1 acts on (p, q) by rotation, we have an explicit parametrisation of the cylinders in phase space given by

$$\begin{aligned} (p_1, q_1, p_2, q_2)(s, \phi; f) &= \\ &(\sqrt{\pi_1} \cos \phi, \sqrt{\pi_1} \sin \phi, (\pi_3 \cos 2\phi + \pi_4 \sin 2\phi)/\pi_1, \sigma(\pi_3 \sin 2\phi - \pi_4 \cos 2\phi)/\pi_1). \end{aligned}$$

The arguments $(s; f)$ for all π_i have been suppressed. This is the local trivialisation of the bundle defined by the regular values of the energy momentum map.

4.2 Energy–momentum mapping

The following results on the structure of the bifurcation diagram for the $1 : \pm 2$ resonance were already described by Henrard [22]. However, his discussion of $\sigma = -1$ was incomplete. Also see Schmidt and Sweet [31], Henrard [23] and Sweet [32] for a more general setting.

Theorem 3. *The critical values of the energy–momentum mapping are contained in the set given by the line $h = h_2$ and the cubic curve*

$$[h_2, h - h_2] = \frac{\sigma}{2}(t - 2\lambda)[3t - 2\lambda, t^2]/c^2 .$$

For $t = 0$ the curve and the line $h = h_2$ are tangent at $[h_2, h - h_2] = \sigma[2\lambda^2, 0]/c^2$.

For $t = 4\lambda/3$ the curve has a cusp at $[h_2, h - h_2] = -2\sigma[9\lambda^2, 8\lambda^3]/27/c^2$.

For $t = 2\lambda$ the curve intersects the line $h = h_2$ transversely in the origin.

Proof. Eliminating π_3 in relation (3.5) by using the Hamiltonian gives the polynomial Q defined in the previous section in (4.6). Tangencies of the reduced Hamiltonian with the reduced phase space are given by the double roots of the cubic polynomial Q . Equating coefficients in $-\sigma Q(z)/(2c^2) - (z-r)^2(z+\sigma t^2/(2c^2)) = 0$ gives the parametrisation of the cubic discriminant surface where $\pi_1 = r = \sigma t(t - 2\lambda)/c^2$. A second solution branch with $r = 0$ and $h = h_2$ for which $h_2 = \sigma(4\lambda^2 - t^2)/2/c^2$ gives a straight line of critical values. \square

The characteristic feature of the curve of critical values of the energy–momentum mapping is that it always has a tangency with the straight line at $t = 0$. However, the cusp is below the line $h = h_2$ for $\sigma\lambda > 0$, and above for $\sigma\lambda < 0$. For $\lambda = 0$ the cusp is on the line.

The transverse intersection at the origin marks the equilibrium point at the origin. The tangency is a bifurcation of periodic orbits that are relative equilibria of the reduced system. This bifurcation collides with the equilibrium point at the passage through resonance when $\lambda = 0$.

Because $\pi_1 \geq 0$ the part of the discriminant locus given by $t \in [0, 2\lambda]$ is not part of the bifurcation diagram for $\sigma = 1$; similarly for $\sigma = -1$ it is the complement. Since $\pi_2 = \sigma(h_2 - \pi_1)/2 \geq 0$ and $\pi_1 \geq 0$ only the part of $h = h_2$ with $h_2 \geq 0$ is part of the bifurcation diagram; similarly for $\sigma = -1$ it is the complement.

For $\sigma = 1$ the piece of the straight line between the transverse intersection and the tangency is a stable relative equilibrium, beyond the tangency it is unstable. The type of the bifurcation is determined by the multiplicity of the preimage of the part of the curve beyond the tangency. The solution for π_i when (h, g) are on the cubic curve is given by

$$\pi = \left(\frac{\sigma}{c^2}t(t - 2\lambda), \frac{(t - 2\lambda)^2}{4c^2}, \pi_1 a \frac{t - 2\lambda}{2c^2}, \pi_1 b \frac{t - 2\lambda}{2c^2} \right) .$$

A point in the pre–image is given by $p_1 = p_2 = q_2 = 0$ and $\pi_1 = q_1^2/2$. The flow of H_2 acting on this point gives all points in the pre–image. This is true for both signs of σ . Hence this bifurcation always is a period doubling bifurcation.

The two branches emanating from the elliptic equilibrium (EE) at the origin are always elliptic (they are the nonlinear normal modes). For $\sigma = 1$ one of them stays stable; while the other one loses stability in a supercritical period doubling bifurcation (supPD), and creates another elliptic relative equilibrium with twice the period. For $\sigma = -1$ one of them disappears in the centre–saddle bifurcation (SC), while the other one collides with a hyperbolic relative equilibrium in a subcritical period doubling bifurcation (subPD) and only one hyperbolic relative equilibrium (with half the period of the previous hyperbolic relative equilibrium) remains. When λ passes through zero, the rôle of the two elliptic branches emanating from the equilibrium is exchanged.

Because $\sigma = -1$ gives a rotated critical curve the tangency now occurs for negative h_2 . The whole plane is in the image of the energy–momentum mapping when $\sigma = -1$. When $\lambda = 0$ the only critical values are those on the ray $h = h_2$ with $h_2 \leq 0$. This is the case studied in [16, 17] which has fractional monodromy. Our unfolding shows that at the endpoint of the ray “half a swallowtail” develops when the resonance is detuned. By continuity, encircling this whole structure and crossing the hyperbolic line $h = h_2$ for sufficiently large negative h_2 will give the same fractional monodromy. In conclusion we have shown

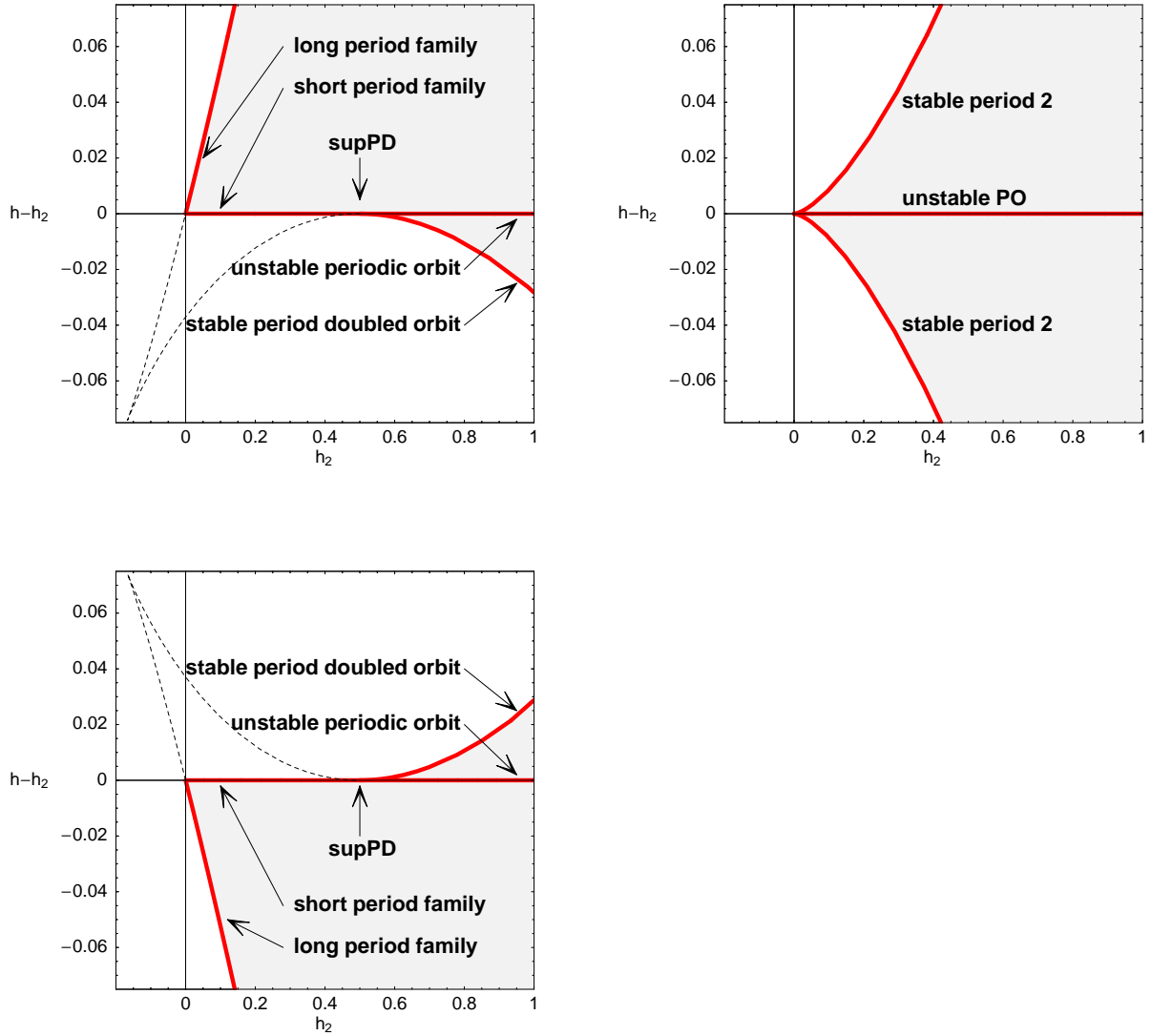


Figure 5: Image of the energy–momentum mapping for 1:2 resonance with $c = 1$, $\lambda = 1/2$ (top left), $\lambda = 0$ (top right), $\lambda = -1/2$ (bottom). Critical values are shown as thick red lines. Dotted lines are part of the discriminant locus, but are outside the image of the energy–momentum mapping (shaded), which is only to the right of the origin, bounded by the thick lines. The supercritical period doubling bifurcation is indicated by supPD.

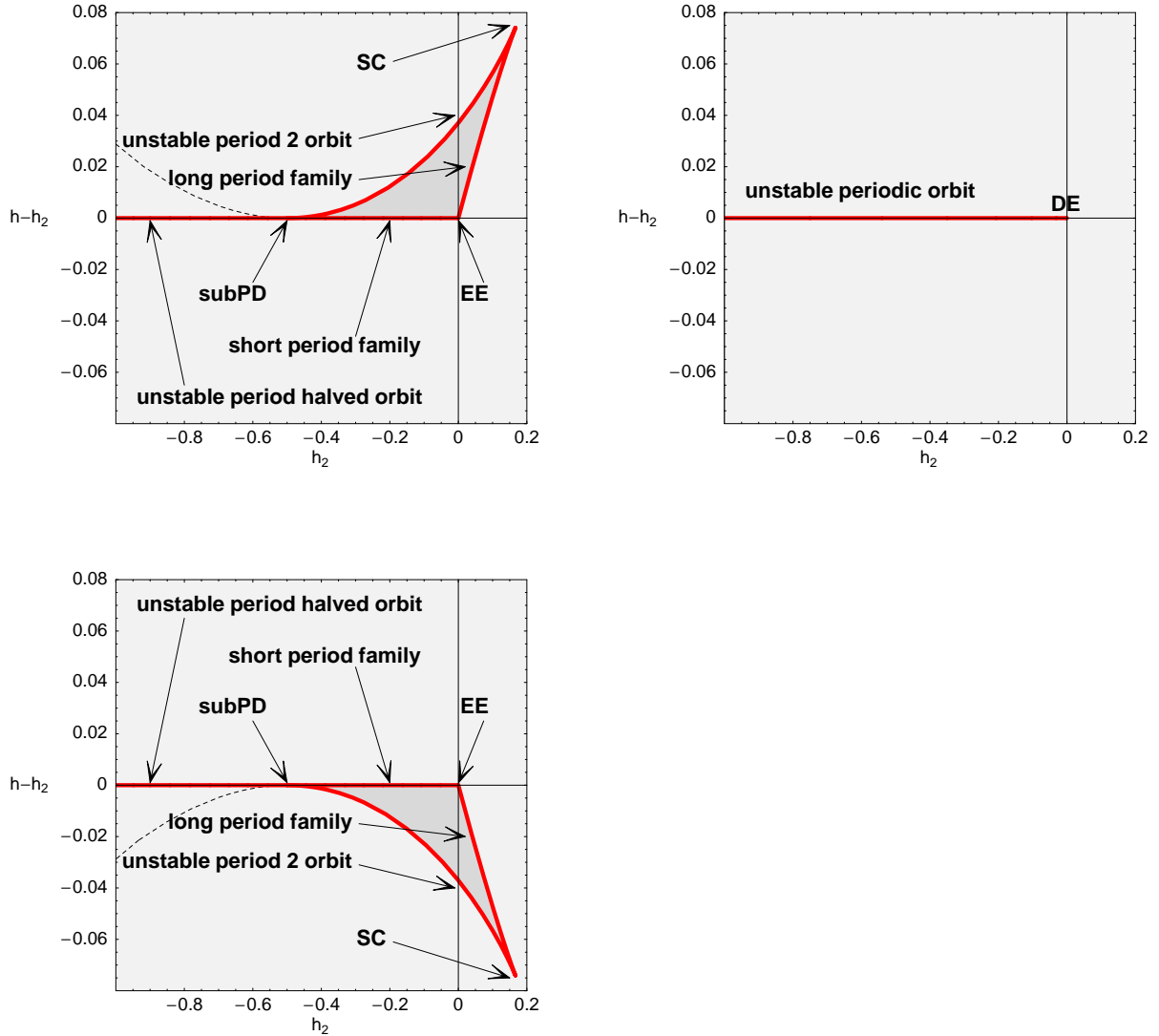


Figure 6: Image of the energy–momentum mapping for the 1:–2 resonance with $c = 1$, $\lambda = 1/2$ (top left), $\lambda = 0$ (top right), $\lambda = -1/2$ (bottom). Critical values are shown as thick red lines. Dotted lines are part of the discriminant locus, but not critical values of the energy–momentum mapping. The whole plane is the image of the energy–momentum mapping. The preimage in the dark shaded region due to detuning lifts to one two–torus \mathbb{T}^2 and a cylinder (figure 3 middle), whereas it is one cylinder otherwise (figure 3 top). Subcritical period doubling bifurcation, centre–saddle bifurcation, the elliptic equilibrium and the degenerate equilibrium are indicated by subPD, SC, EE and DE.

Theorem 4. *The unfolding of the 1:2 resonance shows that nearby there is a supercritical period doubling bifurcation that passes through the equilibrium at resonance. The unfolding of the 1:−2 resonance shows that nearby there is a subcritical period doubling bifurcation and a centre–saddle bifurcation that pass through the equilibrium at resonance. The unfolding of the 1:−2 resonant equilibrium point has fractional monodromy.*

The proof of the last statement is deferred to Section 5.

4.3 Perturbation analysis

The equilibrium remains at the origin because the perturbation consists of higher order terms. Persistence of the periodic orbits and their bifurcations is straightforward. The Diophantine 2–tori will persist, provided that the Kolmogorov condition or iso–energetic non–degeneracy condition holds, see the next sections. For $\sigma = -1$ we will show that the iso–energetic non–degeneracy condition is violated along a line, while the Kolmogorov condition holds everywhere. Similar to the focus-focus case [15], this can be considered to be an effect of the monodromy of the equilibrium.

5 Monodromy

The period of the reduced flow can be computed from

$$\dot{\pi}_1 = \{\pi_1, \mathcal{H}(\pi)\} = \{\pi_1, \lambda\pi_1 + c\pi_3\} = 2c\pi_4.$$

Fixing $\mathcal{H} = \Delta h$ and using (1.3), π_4^2 becomes a polynomial in π_1 . Using $d\pi_1 = w dt$ the period integral is defined on the curve

$$\Gamma = \{(w, \pi_1) \mid w^2 = Q(\pi_1) = 2\sigma c^2 \pi_1^2 (h_2 - \pi_1) - 4(\Delta h - \lambda\pi_1)^2\}.$$

It is given by

$$T(h_2, \Delta h) = \oint_{\gamma} \frac{d\pi_1}{w}.$$

For the compact case $\sigma = 1$ the meaning of this integral is clear. We now focus on the case $\sigma = -1$. A major problem in the non-compact case is to even define what is meant by period, rotation number, and action. Our approach is a simplified version of [29]. Assuming that there are no other critical points on the separatrix, we can split the dynamics into two parts: singular dynamics near the critical point and regular dynamics near the separatrix but away from the critical point, see figure 7.

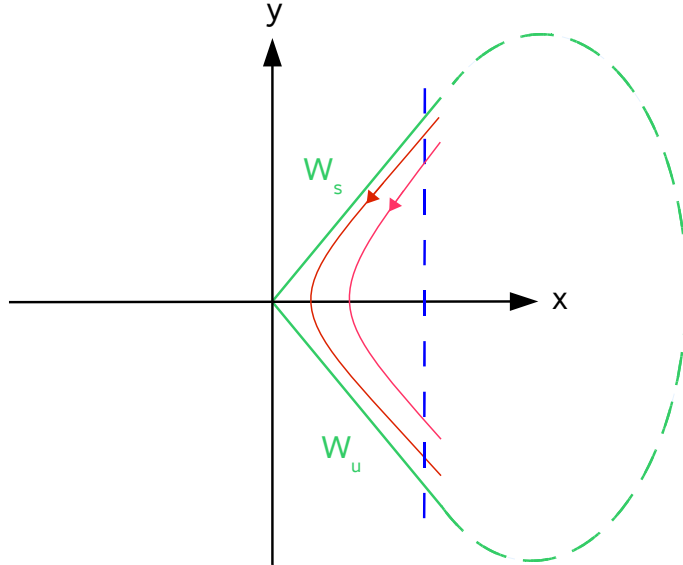


Figure 7: Schematic representation of the dynamics for $\sigma = -1$ close to the separatrix of the singular point at the origin. The green dashed curve indicates the continuation of the stable and unstable manifold of the singular point when compactified.

Assuming that the system has compact invariant tori near the separatrix the contribution of the dynamics far away from the equilibrium is some bounded function with smooth dependence on the initial conditions as long as we stay on the same “side” of the separatrix. This function contains the symplectic invariants of [29], but we are going to completely neglect it. As in [29], the closer we get to the critical value, the main contribution to the period comes from dynamics near the critical point. This contribution diverges in a characteristic way. It is this universal behaviour that we are interested in. For a hyperbolic point the period diverges logarithmically. Our equilibrium is not hyperbolic. Instead we find that the period diverges algebraically. There is one additional trick, which has first been used in [12]. Instead of integrating along the orbit until it leaves a neighbourhood of the critical point, we integrate until the orbit reaches infinity. Thus the integral involved becomes nice namely, a complete elliptic integral. The difference between integrating up to some arbitrary cut-off point and integrating to infinity is a bounded smooth function, which can be neglected. This becomes clear when considered from the point of view of algebraic geometry. The frequency map is given by integrals of holomorphic one-forms over cycles on a complex affine elliptic curve. After adding the point at infinity to make the affine elliptic curve a compact elliptic curve in projective space, cycles that go to infinity on the affine curve are now compact. After this compactification the integral of the holomorphic one form over the compact cycle gives the frequency map. The contribution near the point at infinity is smooth. The asymptotics of the frequency map near the equilibrium point is obtained from the contribution of the cycle near the equilibrium point. This behaviour is unchanged by adding higher order terms to the Hamiltonian. This is the reason why our analysis gives the asymptotic behaviour for all completely integrable systems with the same normal form up to order three.

The parameter c can be removed by the scaling $(\pi_1, h_2, \Delta h) \rightarrow 1/c^2(\pi_1, h_2, \Delta h)$ (similar to the scaling in section 2). The cycle γ extends around the largest real root of w and infinity. This root has the same sign as Δh . For values $(h_2, \Delta h)$ near the line $h = h_2$ there are three real roots. The period integral is finite everywhere except when approaching the critical values along the line $h = h_2$, $T(h_2, 0) = \infty$ for $h_2 < 0$. Even though the reduced motion is unbounded, the time it takes to reach ∞ is finite. This explains why we can treat everything formally as if we were in the compact case.

To compute the rotation number we can either differentiate the action A (see below) with respect to h_2 , or derive the differential equation for dynamics in the fibre. We will pursue the latter.

The S^1 -action makes each cylinder a principal S^1 -bundle, with vertical direction along the fibre. Singling

out a horizontal direction amounts to defining a connection. While an angle in the fibre given by

$$\Theta = \arg z_1$$

is not well-defined, the 1-form $d\Theta$ does define a principal connection simultaneously on all cylinders. The formula $\{\Theta, H_2\} = 1$, however, can still be used since it only involves derivatives. The Poisson brackets with Θ , which describe the dynamics in the fibre in phase space are computed to be

$$\{\Theta, \eta\} = 1, \quad \{\Theta, \pi_1\} = 1, \quad \{\Theta, \pi_3\} = \pi_3/\pi_1.$$

Thus the dynamics of Θ generated by \mathcal{H} is given by

$$\Theta' = \{\Theta, \mathcal{H}\} = \{\Theta, \lambda\pi_1 + c\pi_3\} = \lambda + c \frac{\pi_3}{\pi_1} = \lambda + \frac{\Delta h - \lambda\pi_1}{\pi_1} = \frac{\Delta h}{\pi_1}.$$

For later use we define an integral that describes the variation of Θ when this dynamics in the base completes a full cycle. Changing the integration from dt to $d\pi_1$ and integrating over a period T gives the winding number as

$$W(h_2, \Delta h) = \frac{1}{2\pi} \oint_{\gamma} \frac{\Delta h}{\pi_1} \frac{d\pi_1}{w}. \quad (5.7)$$

We call this integral the winding number, because it measures the (fractional) monodromy of the system.¹ Note that this is not the rotation number of \mathcal{H}_3 , because \mathcal{H} and \mathcal{H}_3 differ by H_2 . This winding number integral (5.7) has a pole at $\pi_1 = 0$. The residue of this pole is $\frac{1}{4\pi} i \operatorname{sgn} \Delta h$. This integral shares many properties with the one discussed in [17]. However, our integral only describes the dynamics near the resonance, while the integral in [17] the terms added for compactification also play a role. The singular behaviour near the equilibrium, however, is the same.

As already mentioned, for the computation of the rotation number of the full Hamiltonian (3.4) the term H_2 needs to be included. The rotation number of the Hamiltonian without this term is what we defined to be the winding number in the previous paragraph. The equations of motion of the two Hamiltonians differ by 1, which originates from $\{\Theta, H_2\} = 1$. Therefore the dynamics of Θ generated by the full Hamiltonian \mathcal{H}_3 is given by

$$\dot{\Theta} = \{\Theta, \mathcal{H}_3\} = 1 + \frac{\Delta h}{\pi_1}.$$

Changing the integration from dt to $d\pi_1$ and integrating over a period T then gives the rotation number

$$2\pi R(h_2, \Delta h) = T(h_2, \Delta h) + 2\pi W(h_2, \Delta h).$$

The period integral has logarithmic singularities. Therefore R does as well. For W the situation is not so obvious.

In order to understand the behaviour of the integrals near the origin we perform the scaling $\pi_1 = \varrho^2 z$ and introduce scaled parameters

$$(h_2, \Delta h, \lambda) \rightarrow (\varrho^2 h_2, \varrho^3 \Delta h, \varrho \lambda).$$

This is similar to the scaling done in section 2, but we repeat these steps here because we want to interpret this scaling as choosing a new co-ordinate system on the image of the energy-momentum map. This scaling shows that the winding number is independent of the ‘‘radius’’ ϱ . In order to study the behaviour of W when the origin is encircled we therefore introduce weighted polar co-ordinates in the image of the momentum map by

$$(h_2, \Delta h, \lambda) = (\varrho^2 \cos \theta, \varrho^3 \sin \theta, \varrho \tilde{\lambda}).$$

¹Even though a winding number is usually an integer, we will use the term for the function W that changes by a (half-) integer over a cycle around the origin of the energy-momentum map.

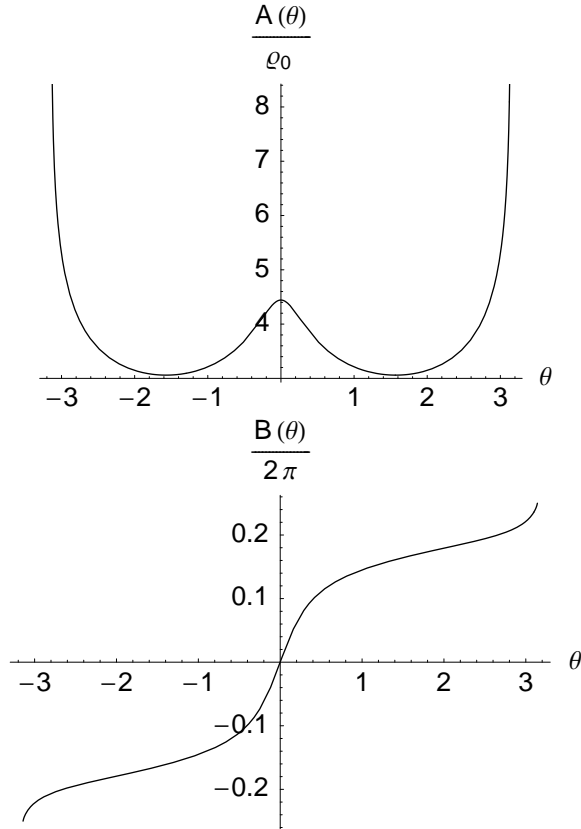


Figure 8: Period $T = A/\rho$ and winding number $W = B/2\pi$, see (5.8), as a function of $\theta \in [-\pi, \pi]$ for fixed $\varrho = \varrho_0$ and $\lambda = 0$. T is even and periodic with logarithmic divergence at $\theta = \pm\pi$. W is odd and continuous, but not periodic: it increases by $1/2$ when θ completes a circle.

The transformation from $(h_2, \Delta h)$ to new variables near the origin of the momentum map $(u, v) = \varrho^{5/2}(\cos \theta, \sin \theta)$ is C^0 at the origin and C^∞ everywhere else. With this notation the crucial integrals become

$$T(h_2, \Delta h) = \frac{1}{\varrho} A(\theta), \quad 2\pi W(h_2, \Delta h) = B(\theta). \quad (5.8)$$

If the degenerate equilibrium is approached on a curve in parameter space $(h_2, \Delta h)$ with non-vanishing derivative at the origin, the leading order term of T reads $|\Delta h|^{-1/3}$. Along the line $\Delta h = 0, h_2 > 0$, we find $1/\sqrt{h_2}$ as leading order term of T . So in our two-degree of freedom system the leading order behaviour of the period T as a function of $(h_2, \Delta h)$ depends on how the equilibrium is approached. This is in contrast to one degree of freedom systems where the energy h is the only parameter.

The integrals A and B are defined on the curve

$$\tilde{\Gamma} = \{(z, w) : \tilde{w}^2 = 2\sigma z^2(\cos \theta - z) - 4(\sin \theta - \tilde{\lambda}z)^2\}$$

where

$$dA(\theta) = \frac{1}{\tilde{w}} dz, \quad dB(\theta) = \frac{\sin \theta}{z\tilde{w}} dz.$$

The parameter $\tilde{\lambda}$ must be chosen sufficiently small so that there are no critical values encountered on the loop around the origin in the $(h_2, \Delta h)$ plane. The plots of the functions A and B (i.e. of T and W on a loop around the origin with $\varrho = \text{const}$) are shown in figure 8.

The period T diverges algebraically as $1/\varrho$ when the origin is approached. This is due to the fact that the equilibrium is a degenerate singularity: specifically, the value of the Hessian of the cubic integral at

the critical point (i.e. the origin) vanishes identically. The winding number is independent of the distance from the origin ρ . The period diverges logarithmically when $\theta \rightarrow \pm\pi$. This is the usual divergence when approaching a hyperbolic periodic orbit. The winding number is only a continuous function of θ . It is not differentiable. Surprisingly, the winding number is not a periodic function of θ , even though its defining integrand is.

We now prove that the increase in values of W (or B) when we let $\theta \in [-\pi, \pi]$ is indeed as suggested by figure 8. First of all observe that B is an odd function, so we can restrict to $\theta \geq 0$. For $\lambda = 0$ the polynomial \tilde{w}^2 has one non-negative real root and two roots with non-positive real part (which may be real or complex). For $\theta = 0$ these are $(1, 0, 0)$ and for $\theta = \pi$ these are $(0, 0, -1)$. There is a double root for $\theta = 0$. But since we always integrate from the largest root onwards this does not concern us (there is another collision of roots, but again it is not in the physically allowed region). Thus the function $B(\theta)$ is smooth for $\theta \in (-\pi, \pi)$. The double root at 0 for $\theta = \pi$ is at the boundary of the integration interval, so care needs to be taken when evaluating B . At first sight it looks like $B(\pi) = 0$ (which would also be required for a periodic odd function). However, we will now show that $B(\theta)$ is not periodic, but instead has non-zero $\pi/2$ value at $\theta = \pi$. Since B is odd therefore $B(-\pi) = -\pi/2$ and $B(\pi) - B(-\pi) = \pi$: the value of B increases by π when θ traverses $[-\pi, \pi]$.

Lemma 5.

$$\lim_{\theta \rightarrow \pm\pi^\mp} B(\theta) = \pm\pi/2 + \arcsin(\sqrt{2}\lambda)$$

Proof. We consider the limit to $+\pi$ from the left first. When $\theta \rightarrow \pi$ we can treat $\delta = \sin\theta$ as a small parameter. The colliding roots behave like δ , thus we scale $z = y\delta$ and find

$$dB = 1/(y\sqrt{-2y^2(\cos\theta - y\sin\theta) - 4(1 - \lambda y)^2})dy$$

The root that limits to $z = -1$ in the new variables tends to $-\infty$ when $\delta \rightarrow 0$. The other two roots of opposite sign tend to non-zero values. Denote these roots (for any small value of δ) by $y_\infty < y_- < y_+$. The integration interval now is $[y_+, \infty)$. In order to regularize the square root singularity of the integrand at y_+ and also make the lower integration boundary independent of δ we introduce new variables by $y = y_+ + u^2$. Now the integrand is a smooth function of u and δ uniformly over the integration interval. We now can compute the Taylor series in $\theta - \pi$. The first term gives the value of B at $\theta = \pi$ as

$$B(\pi) = 2 \int_0^\infty \frac{\sqrt{2} du}{(u^2 + y_+) \sqrt{2y_+ + 4\lambda(1 - \lambda y_+) + u^2(1 - 2\lambda^2)}}$$

Since the integrand is even function of u , the interval of integration can be extended to $[-\infty, \infty]$, absorbing one factor of 2. Direct evaluation of the integral gives the stated result. The computation is similar for $B(\pi)$, except that now δ is negative which changes the sign of the constant term in the result, but not the λ -dependent part. As a result the difference $B(\pi) - B(-\pi) = \pi$ is independent of λ . \square

For later use we also record the following

Lemma 6. *The function $B(\theta)$ for $\lambda = 0$ is strictly monotonic.*

Discussion In the appendix we give the expression for B' in terms of Legendres complete standard integrals K and E . Using these formulas it can be numerically unambiguously verified that B' does not have a zero. The function B' can be plotted with any standard symbolic algebra program. We find $B' > 0.15$, so it is bounded away from zero such that only a few digits of accuracy are needed. Thus round-off errors in the computation do not play a role. We have not been able to find an analytic proof yet. *end of discussion*

To establish monodromy is now simply a matter of finding an expression for the actions $I = (I_1, I_2)$ for the integrable system. One action I_2 is trivial, namely the generator of the S^1 symmetry. Set $I_2 = h_2$. The non-trivial action I_1 of the system (or more precisely, its leading order term near the equilibrium) contains some terms that depend smoothly and periodically on θ . However, it has a term Wh_2 , which changes by $\frac{1}{2}$ over a cycle around the origin, see Lemma 5. Thus I_1 changes by $\frac{1}{2} I_2$ after traversing this loop. This behaviour is called fractional monodromy [27].

Lemma 7. *The non-trivial action I_1 of the 1:–2 resonance has the form*

$$I_1(h_2, \Delta h) = \frac{3}{2} \frac{\Delta h}{2\pi} T - h_2 W.$$

It is discontinuous across the singular value at $\Delta h = 0$ and it changes by $h_2/2 = I_2/2$ along a loop around the origin.

Proof. For the computation of the action of the reduced system two canonically conjugate functions whose Poisson bracket equals one are needed. It is easy to check that

$$\left\{ \cos^{-1} \frac{\pi_3}{\sqrt{\pi_1^2 \pi_2}}, \pi_2 \right\} = 1$$

before introducing η in the Poisson structure. Now the action is given by

$$I_1(h_2, \Delta h) = -\frac{1}{2\pi} \oint \cos^{-1} \left(\frac{\pi_3}{\sqrt{\pi_1^2 \pi_2}} \right) d\pi_2.$$

Integration by parts and changing the integration variable to $\pi_1 = h_2 + 2\pi_2$ gives

$$I_1(h_2, \Delta h) = \frac{\Delta h}{2\pi} \oint \left(\frac{3}{2} - \frac{h_2}{\pi_1} \right) \frac{d\pi_1}{w}$$

and the result follows. □

The formula of Lemma 7 should be compared to the analogous expression for a focus-focus point, which is $I_1 = J_1 T - J_2 W$ where J_i are the co-ordinates from the Eliasson normal form [29]. The two formulas are surprisingly similar, even though the corresponding equilibria are quite different.

Note that the remarkable formula of Lemma 7 can also be read as a decomposition of the angle change $2\pi W$ into a geometric phase (namely the action) and a dynamic phase (the term proportional to T). In many cases simple relations like this can be found for the change of angle in the fibre computed from quantities in the base, see, e.g., Montgomery [26].

For us the most important aspect of Lemma 7 is that together with Lemma 5 it immediately implies the following monodromy theorem, complementing the work of [27, 17].

Theorem 8. *The Hamiltonian system describing the 1:–2 resonance has fractional monodromy $\frac{1}{2}$.*

Let us point out the philosophy in our approach once more. Following Duistermaat [10] classical monodromy can be understood by considering the period lattice, or equivalently, following Cushman [9] the rotation number of the system. Following Zhilinskiĭ [35] another way to think of Hamiltonian monodromy is in terms of lattice defects in the associated quantum analog. In the present case the rotation number is singular at the critical values of the energy-momentum map along the line $h = h_2$, and the fibres are unbounded. This makes it hard to speak about continuing the period lattice or rotation number around the origin (the degenerate critical point corresponding to the equilibrium). The first papers discovering fractional monodromy [27] used a geometric approach. Later [16] a rescaled time was used in order to “remove” the blowup of T . Our approach is similar to this, in that we are dealing with a similar type of elliptic integrals. There are two differences. Firstly, in the proof of monodromy we directly consider the actions of the system. Even when the rotation number is singular, the action can always be chosen continuous across separatrices (up to integer factors counting the number of tori, etc.). In our case the action can be made continuous at any point, but globally it is not single valued, due to the contribution of W . It seems that in general the actions are the more “robust” objects that are well suited for this type of consideration. Secondly, instead of compactifying the Hamiltonian by adding higher order terms we directly treat the non-compact situation, by only considering dynamics near the singularity. This is inspired by the approach of San Vu Ngoc [29] to the symplectic invariants near focus-focus points. Our main new results are presented in the next section, where we consider the derivatives of the functions A and B in order to study the non-degeneracy condition of the KAM theorem.

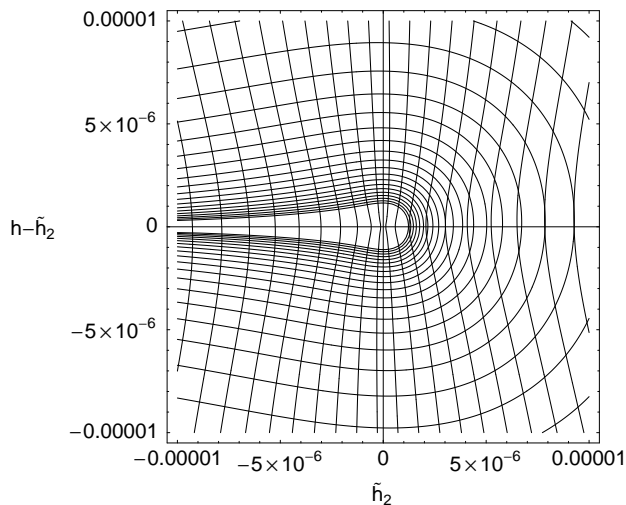


Figure 9: Illustration of the condition on vanishing twist in the 1 : -2 resonance. The twist condition is violated where the lines of constant h are tangent to the contour lines of $R(h_2, \Delta h)$ which is the case for $\Delta h = 0$ and $\tilde{h}_2 > 0$. $\tilde{h}_2 = \varrho^3 \cos \theta$.

6 Frequency Map

The results in this and the following section are valid at the bifurcation $\lambda = 0$ only. For perturbation theory we have to consider the actual rotation number R not just the less singular winding number part. To study the derivatives of R and the frequencies it is best to use the scaled forms of the integrals. Only the leading term when $\varrho \rightarrow 0$ is relevant. Inverting $\partial(h_2, h)/\partial(\varrho, \theta)$ gives

$$\frac{\partial \varrho}{\partial h_2} = -\Delta \varrho^2 \sin \theta + O(1/\varrho), \quad \frac{\partial \theta}{\partial h_2} = -2\Delta \varrho \cos \theta + O(1/\varrho^2),$$

where the determinant of the transformation is

$$\Delta = \left| \frac{\partial(\varrho, \theta)}{\partial(h_2, h)} \right| = \frac{2}{\varrho^4(5 - \cos 2\theta)}.$$

Theorem 9. (*Vanishing Twist*) *The isoenergetic non-degeneracy condition is violated on a line emerging from the critical value at the origin of the 1:-2 resonance. Namely the function $R(h_2)$ has a critical value at $h_2 = h$ for $\lambda = 0$.*

Proof. Computing the derivative of $2\pi R = A(\theta)/\varrho + B(\theta)$ after scaling gives

$$2\pi \frac{\partial R}{\partial h_2} = -\frac{A}{\varrho^2} \frac{\partial \varrho}{\partial h_2} + \left(\frac{A'}{\varrho} + B' \right) \frac{\partial \theta}{\partial h_2} = \Delta(A \sin \theta - 2A' \cos \theta) + O(1/\varrho^3)$$

For $\lambda = 0$ the function A is even in θ and therefore the leading order term vanishes at $\theta = 0$. For $\lambda \neq 0$ the origin becomes a non-degenerate elliptic fixed point, and the vanishing twist will instead be present near the centre-saddle bifurcation [12], see the bifurcation diagram figure 6. \square

A graphical illustration of the condition on vanishing twist is given in figure 9. The frequencies of the system are

$$\omega_1 = 2\pi/T, \quad \text{and} \quad \omega_2 = 2\pi R/T = 1 + 2\pi W/T.$$

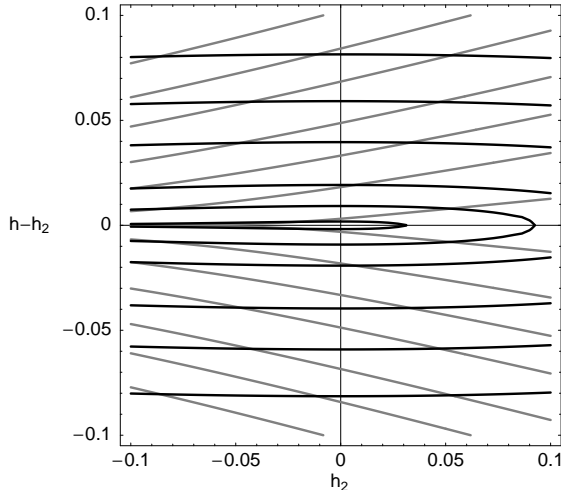


Figure 10: The non-violation of the Kolmogorov condition means the frequencies plotted in the image of the energy-momentum mapping give a “nice” co-ordinate system. The contour lines of ω_2 are black, the ones of ω_1 gray.

Theorem 10. *The Kolmogorov non-degeneracy condition*

$$\left| \frac{\partial \omega}{\partial I} \right| \neq 0$$

is satisfied at every point in a neighbourhood of the origin of the 1:–2 resonance.

Proof. The determinant is the product of three determinants

$$\left| \frac{\partial \omega}{\partial I} \right| = \left| \frac{\partial \omega}{\partial(\varrho, \theta)} \right| \left| \frac{\partial(\varrho, \theta)}{\partial(h_2, h)} \right| \left| \frac{\partial(h_2, h)}{\partial(I_1, I_2)} \right|$$

The middle one is Δ , and hence non-zero outside the origin. Since $h_2 = I_2$ the last one reduces to $-\partial h / \partial I_1 = -\omega_1$ which is non-zero outside the critical values. The non-trivial first determinant is (exactly!) given by

$$\left| \frac{\partial \omega}{\partial(\varrho, \theta)} \right| = \left| \begin{pmatrix} 2\pi/A & -2\pi\varrho A'/A^2 \\ B/A & \varrho(B'A - A'B)/A^2 \end{pmatrix} \right| = 2\pi\varrho \frac{B'}{A^2}.$$

In Lemma 6 we have shown that $B(\theta)$ is monotonic, see figure 8. This completes the proof.

Collecting the above results we find that

$$\left| \frac{\partial \omega}{\partial I} \right| = -(2\pi\varrho)^2 \frac{B'}{A^3} \Delta$$

Notice that this diverges like $1/\varrho^2$ when approaching the origin away from $\theta = \pm\pi$. When $\theta \rightarrow \pm\pi$ for fixed ϱ , however, the determinant approaches zero because both, A and B' diverge logarithmically. \square

In this section we only considered the case without detuning, $\lambda = 0$. However, using the analysis for period doubling in [24] and for the centre-saddle bifurcation in [12] it is straightforward to get a qualitative understanding of vanishing twist for $\lambda \neq 0$ as well. For $\sigma = +1$ no vanishing twist is forced by the bifurcation. For $\sigma = -1$ the cusp of the centre-saddle bifurcation will produce a curve emanating from it along which the twist condition is violated. For $\lambda \rightarrow 0$ this curve will locally coincide with $\Delta h = 0$ as predicted here. Combining the images of the energy-momentum map for different parameters λ into a three-dimensional picture there will therefore be a surface along which the twist condition is violated. To our knowledge the Kolmogorov condition has not been investigated near these bifurcations.

Acknowledgements

HH thanks Hans Duistermaat for helpful discussions. RHC, HRD and HH thank the Centre Interfacultaire Bernoulli at the EPF Lausanne for its hospitality. This research was partially supported by the European Research Training Network *Mechanics and Symmetry in Europe* (MASIE), HPRN-CT-2000-00113. HRD acknowledges partial support by a research fellowship of the Leverhulme trust.

A Standard Form of the Integrals A , B , A' , and B'

Here we present the main elliptic integrals in Legendre normal form for the cases of three real and one real root of \tilde{w}^2 . This can be avoided using a Landen transformation [6] but since this doesn't simplify the Legendre normal forms we refrained from doing so. We denote the real roots by $a > b > c$ and the complex conjugate ones by b and \bar{b} .

$A(\theta)$ is simply given by

$$A(\theta) = \sqrt{2} g K(m) \tag{A.9}$$

where

$$g = \frac{2}{\sqrt{a-c}}, \quad m = \frac{b-c}{a-c}$$

for three real roots and

$$g = \frac{1}{\sqrt{d}}, \quad m = \frac{d+b_1-a}{2d}, \quad d^2 = (\operatorname{Re} b - a)^2 + (\operatorname{Im} b)^2$$

for one real root. The derivative of A is of 2nd kind. For three real roots we find

$$A'(\theta) = \sqrt{2} g [K(m) (u_1 + a u_2) - u_2 (a - c) E(m)] \tag{A.10}$$

with

$$u_1 = \frac{\sin 2\theta}{2D} (\mu^2 \cos \theta - 9), \quad u_2 = \frac{\mu^2 \cot \theta}{4D} (\cos 2\theta - 5),$$

where D is the discriminant of $\tilde{\omega}^2$ given by $D = 2\mu^2 \cos^3 \theta + 27 \sin^2 \theta$. In the case of one real root we have

$$A'(\theta) = \sqrt{2} g [K(m) (u_1 + (a + d) u_2) - 2 d u_2 E(m)]. \tag{A.11}$$

$B(\theta)$ is the elliptic integral of 3rd kind

$$B(\theta) = \sqrt{2} g \sin \theta \left[\frac{K(m)}{b} + \frac{b-a}{ba} \Pi \left(\frac{b}{a}, m \right) \right] \tag{A.12}$$

in the case of three real roots and

$$B(\theta) = \sqrt{2} \frac{g}{a+d} \sin \theta \left[\frac{K(m)}{\alpha} + \frac{\alpha-1}{\alpha(1-\alpha^2)} \Pi \left(\frac{\alpha^2}{\alpha^2-1}, m \right) \right] \tag{A.13}$$

otherwise, where

$$\alpha = \frac{a-d}{a+d}.$$

Its derivative is of 2nd kind. For three real roots we find

$$B'(\theta) = -\sqrt{2} g [K(m) (u_1 + a u_2) - u_2 (a - c) E(m)] \tag{A.14}$$

where

$$u_1 = \frac{\mu^2 \cos \theta}{4D} (\cos 2\theta - 5), \quad u_2 = \frac{3\mu^2}{4D} (2 + \sin^2 \theta).$$

In the case of one real root we finally have

$$B'(\theta) = -\sqrt{2} g [K(m) (u_1 + (a + d) u_2) - 2 d u_2 E(m)]. \tag{A.15}$$

References

- [1] K. T. Alfriend and D. L. Richardson. Third and fourth order resonances in hamiltonian systems. *Celestial Mech.*, 7:408–420, 1973.
- [2] John. V. Breakwell and Jr. Ralph Pringle. Resonances affecting motion near the earth-moon equilateral libration points. In R. L. Duncome and V. G. Szebehely, editors, *AIAA Progress in Astonautics and Aeronautics*, volume 17 of *Methods in Astrodynamics and Celestial Mechanics*, pages 55–74. Academic, 1966.
- [3] H. W. Broer, R. H. Cushman, F. Fassò, and F. Takens. Geometry of KAM tori for nearly integrable hamiltonian systems. *Ergod. Th. & Dynam. Sys.*, 27:725–741, 2007.
- [4] H.W. Broer, S.-N. Chow, Y. Kim, and G. Vegter. A normally elliptic hamiltonian bifurcation. *Z. angew. Math. Phys.*, 44:389–432, 1993.
- [5] H.W. Broer, I. Hoveijn, G. Lunter, and G. Vegter. *Bifurcations in Hamiltonian Systems*, volume 1806 of *Lecture Notes in Mathematics*. Springer-Verlag, 2003.
- [6] Paul F. Byrd and Morris D. Friedman. *Handbook of Elliptic Integrals for Engineers and Scientists*. Springer-Verlag, 2nd revised edition, 1971.
- [7] C. Cotter. *The 1:1 semisimple resonance*. PhD thesis, University of California at Santa Cruz, 1986.
- [8] R. Cushman and J. Sanders. Invariant theory and normal form of hamiltonian vectorfields with nilpotent linear part. In W.F. Langford, F.V. Atkinson, and A.B. Mingarelli, editors, *Oscillation, Bifurcation and Chaos*, volume 8 of *CMS Conference Proceedings*, pages 353–371. AMS, 1987.
- [9] Richard H. Cushman and Larry M. Bates. *Global Aspects of Classical Integrable Systems*. Birkhäuser, 1997.
- [10] J. J. Duistermaat. On global action-angle coordinates. *Comm. Pure Appl. Math.*, 33(6):687–706, 1980.
- [11] J. J. Duistermaat. Bifurcations of periodic solutions near equilibrium points of hamiltonian systems. volume 1057 of *Lecture Notes in Mathematics*, pages 57–105. Springer-Verlag, 1983.
- [12] H. R. Dullin and A. V. Ivanov. Another look at the saddle-centre bifurcation: Vanishing twist. *Phys. D*, 211(1-2):47–56, 2005.
- [13] H. R. Dullin and A. V. Ivanov. Vanishing twist in the hamiltonian hopf bifurcation. *Phys. D*, 201(1-2):27–44, 2005.
- [14] H. R. Dullin, J. D. Meiss, and D. Sterling. Generic twistless bifurcations. *Nonlinearity*, 13(1):203–224, 2000.
- [15] H. R. Dullin and S. Vũ Ngọc. Vanishing twist near focus-focus points. *Nonlinearity*, 17(5):1777–1785, 2004.
- [16] K. Efstathiou. *Metamorphoses of Hamiltonian systems with symmetries*, volume 1864 of *Lecture Notes in Mathematics*. Springer-Verlag, 2005.
- [17] K. Efstathiou, R. H. Cushman, and D. A. Sadovskii. Fractional monodromy in the $1 : -2$ resonance. *Adv. in Math.*, 209:241–273, 2007.
- [18] A. Elipe, V. Lanchares, T. López-Moratalla, and A. Riaguas. Nonlinear stability in resonant cases: a geometrical approach. *J. Nonlinear Sci.*, 11(3):211–222, 2001.
- [19] A. Elipe, V. Lanchares, and A. I. Pascual. On the stability of equilibria in two-degrees-of-freedom hamiltonian systems under resonances. *J. Nonlinear Sci.*, 15(5):305–319, 2005.

- [20] G. Haller and S. Wiggins. Geometry and chaos near resonant equilibria of 3-dof hamiltonian systems. *Phys. D*, 90(4):319–365, 1996.
- [21] H. Hanßmann. *Local and Semi-Local Bifurcations in Hamiltonian Dynamical Systems – Results and Examples*, volume 1893 of *Lecture Notes in Mathematics*. Springer-Verlag, 2007.
- [22] J. Henrard. Periodic orbits emanating from a resonant equilibrium. *Celestial Mech.*, 1(437-466), 1970.
- [23] J. Henrard. Lyapunov’s center theorem for resonant equilibrium. *J. Differential Equations*, 14:431–441, 1973.
- [24] H.R.Dullin and A.V. Ivanov. Rotation function near resonant bifurcations. In A. V. Bolsinov, A. T. Fomenko, and A. A. Oshemkov, editors, *Topological Methods in the Theory of Integrable Systems*. Taylor and Francis, 2005.
- [25] M. Kummer. On resonant hamiltonian systems with finitely many degrees of freedom. *Lecture Notes in Phys.*, 252:19–31, 1986.
- [26] Richard Montgomery. How much does the rigid body rotate? A Berry’s phase from the 18th century. *Amer. J. Phys.*, 59(5):394–398, 1991.
- [27] N. N. Nekhoroshev, D. A. Sadovskii, and B. I. Zhilinskiĭ. Fractional monodromy of resonant classical and quantum oscillators. *C. R. Acad. Sci. Paris*, 335:985–988, 2002.
- [28] N. N. Nekhoroshev, D. A. Sadovskii, and B. I. Zhilinskiĭ. Fractional hamiltonian monodromy. *Ann. Henri Poincare*, 7(6):1099–1211, 2006.
- [29] S. Vũ Ngọc. On semi-global invariants of focus-focus singularities. *Topology*, 42(2):365–380, 2003.
- [30] Jan Sanders. Are higher resonances really interesting? *Celestial Mech.*, 16(4):421–440, 1978.
- [31] D. S. Schmidt and D. Sweet. A unifying theory in determining periodic families for hamiltonian systems at resonance. *J. Differential Equations*, 14:597–609, 1973.
- [32] D. Sweet. Periodic solutions for dynamical systems possessing a first integral in the resonance case. *J. Differential Equations*, 14:171–183, 1973.
- [33] J.C. van der Meer. *The Hamiltonian Hopf bifurcation*, volume 1160 of *Lecture Notes in Mathematics*. Springer-Verlag, 1985.
- [34] H. Waalkens, H. R. Dullin, and P. H. Richter. The problem of two fixed centers: bifurcations, actions, monodromy. *Physica D*, 196:265–310, 2004.
- [35] B. I. Zhilinskiĭ. Hamiltonian monodromy as lattice defect. In *Topology in Condensed Matter*, volume 150 of *Springer Series in Solid-State Sciences*, pages 165–186. Springer-Verlag, 2006.